scientific reports

Check for updates

OPEN

Isorhamnetin inhibits mechanical stress-induced chondrocyte apoptosis through activation of the ROS/SRC/FOXO1 signaling pathway

Jinliang Lai[1,7], Guoqiang Yin[3,7], Fanmao Zhu[2,7], Jishang Huang[2,7], Xinghua Hu[4], Lei Liao[5], Rong Wu[6], Jiayu Tao[6], Shuyue Wang[6], Yang Xiao[6], Yiming Gu[6], Shan Li[6], Jie Zhou[6] & Yadong Yang[2]✉

Intervertebral disc degeneration (IDD), a chronic degenerative disease, is characterized by pain without a satisfactory therapeutic strategy. Excessive mechanical pressure contributes to the pathological development of IDD by inducing chondrocyte apoptosis in the cartilage endplate. Isorhamnetin (ISO) has been shown to have chondroprotective effects by promoting chondrocyte proliferation and inhibiting chondrocyte apoptosis. In this study, we found that mechanical loading could inactivate the SRC/FOXO1 signaling pathway and increase chondrocyte apoptosis, leading to disc degeneration in rats. ISO neutralized mechanical loading-induced chondrocyte apoptosis and attenuated the progression of disc degeneration. However, activation of ROS/SRC/FOXO1 signaling by EPQpYEEIPIYL (EPQ) and H2O2 attenuated the biological effects of ISO on mechanical loading-treated chondrocytes. Therefore, ISO may protect against mechanical loading-induced injury and inhibit chondrocyte apoptosis through the activation of the ROS/SRC/FOXO1 signaling pathway.

Keywords Isorhamnetin, Intervertebral disc degeneration, Endplate chondrocytes, Apoptosis, SRC

Intervertebral disc degeneration (IDD) is an age-related degenerative disease that is considered a cause of neck pain. It imposes a very large health and economic burden on society and severely reduces patients' quality of life[1,2]. A systematic review revealed that more than 68% of people over the age of 40 have typical radiographic changes in IDD[2]. Current treatments for IDD often lead to unsatisfactory results, such as unsuccessful pharmacological interventions, surgery-associated deterioration of disc degeneration, and recurrence after surgery[3].

Intact IVD elements help the cervical spine maintain structural stability[4]. The biological function of the IVD is significantly influenced by the CEP, which plays a critical role in stress distribution and nutrient metabolism[5,6]. It has been reported that apoptosis and structural degeneration of the CEP may contribute to the progression of IDD[7–9]. In particular, CEP cell apoptosis is considered a risk factor for IDD development[10,11]. One study revealed that increased CEP cell apoptosis increases the incidence of IDD[12]. However, the underlying mechanism of CEP cell apoptosis in IDD development remains unclear. The homeostasis of the mechanical loading microenvironment is associated with the stable physiological functions of the IVD. Studies have shown that mechanical loading can control cell behaviors, including apoptosis, which are involved in the occurrence and development of IDD[13,14]. Excessive mechanical loading contributes to IDD pathogenesis[14,15]. In addition, the CEP, as a main participant in spine movement, is particularly susceptible to mechanical loading. Recent findings have shown that excessive mechanical stress significantly contributes to the apoptosis of CEP cells[16,17]. However, the underlying molecular mechanisms are unclear.

[1]Emergency Department, Trauma Center, First Affiliated Hospital of GannanMedical University, Ganzhou 341000, Jiangxi, China. [2]Department of Orthopedics, First Affiliated Hospital of Gannan MedicalUniversity, Ganzhou 341000, Jiangxi, China. [3]Department of Orthopedic Surgery, Ganzhou People's Hospital, Jiangxi MedicalCollege, Nanchang University, Ganzhou 341000, Jiangxi, China. [4]Department of Orthopedics, Xingguo People's Hospital, Ganzhou 341000, Jiangxi, China. [5]Dingnan Second Hospital, Ganzhou 341000, Jiangxi, China. [6]Ganan Medical University, Ganzhou 341000, Jiangxi, China. [7]These authors contributed equally: Jinliang Lai, Guoqiang Yin, Fanmao Zhu and Jishang Huang. ✉email: ydgogai@163.com

Reactive oxygen species (ROS) play crucial roles in connecting mechanical stress to the programmed cell death of chondrocytes[18]. Excessive mechanical stress significantly increases ROS levels inside cells, triggering several downstream pathways that lead to cartilage breakdown. Among these pathways, the nonreceptor tyrosine kinase SRC has attracted increasing interest. SRC acts as a mediator of oxidative stress signaling and controls various cellular functions, such as cytoskeleton remodeling, apoptosis, and changes in gene expression[19]. Notably, SRC promotes apoptosis in chondrocytes partly by influencing Forkhead box protein O1 (FOXO1), a transcription factor that regulates antioxidant defenses, mitochondrial balance, and cell survival[20]. When FOXO1 is inactivated because of mechanical stress, chondrocyte apoptosis accelerates, whereas its activation helps prevent cartilage deterioration.

Isorhamnetin (ISO), a plant flavonoid compound derived from *Hedysarum Multijugum Maxim*, has been shown to reduce the progression of osteoarthritis and exert a cartilage-protective effect[21,22]. In addition, ISO has an antiosteoarthritic effect by alleviating interleukin 1β (IL-1β)-induced cartilage inflammation and tissue damage[23]. Recently, ISO was shown to inhibit pathological changes in rheumatoid arthritis by regulating the SRC/ERK/CREB signaling axis[24]. Similarly, by modulating α-enolase expression in cardiomyocytes, ISO attenuates isoprenaline-induced myocardial injury[25]. EPQpYEEIPIYL (EPQ), a small-molecule peptide, acts as an SRC activator and has demonstrated the ability to specifically identify the Src homology-2 structural domain, resulting in strong binding affinity[26]. To further investigate the protective activity of ISO, this study aimed to investigate whether ISO inhibited excessive mechanical loading-induced chondrocyte apoptosis by mediating the expression of ROS/SRC/FOXO1 signaling.

Materials and methods

Network Pharmacology

Based on the keyword "*Hedysarum Multijugum Maxim*", all the chemical constituents in the Chinese herb Astragalus were searched in the TCM systematic pharmacology database and analytical platform (TCMSP, http://lsp.nwu.edu.cn/). As reported previously, compounds with higher activity were further screened under the following conditions: drug likeness (DL) ≥ 0.15, BBB ≤ − 2.0, oral bioavailability (OB) ≥ 20%, 100 ≤ molecular weight ≤ 500, and log*P* < 5. In addition, information on isorhamnetin, such as the PubChem ID, CAS, and structural formula, was acquired from the PubChem database (https://pubchem.ncbi.nlm.nih.gov/). The Swiss Target Prediction Web Server (http://www.swisstargetprediction.ch/) was used to forecast the targets of the chemical compositions. The targets related to IDD were obtained from the GeneCards database (https://www.genecards.org/). The keyword "intervertebral disc degeneration" and "*Homo sapiens*" were used to search for targets. An analysis platform and an Excel spreadsheet exported from the database were used to identify shared targets between compounds and IDD through comparison. A protein crosstalk network was constructed using Cytoscape 3.7.2 (https://cytoscape.org/). Diagrams were generated with Venny: Oliveros, J.C. (2007–2015) Venny. The online tools were employed to create comparative diagrams (https://bioinfogp.cnb.csic.es).

Animal models

This study (GMU202110) was licensed by the Animal Ethics Committee of Gannan Medical University in accordance with the Declaration of Helsinki Principles. The bipedal rat animal model constructed in this study was reviewed and approved by the Animal Ethics Committee of Gannan Medical University. All experiments were performed in accordance with the ARRIVE guidelines and relevant institutional and national regulations. Internationally recognized guidelines for the care and use of laboratory animals (EEC Directive of 1986; 86/609/EEC) were referenced for this study. All the rats were acclimatized for one week in an SPF-rated environment. Adequate food and water and a 12-hour light–dark cycle were provided.

A total of 48 4-week-old male Sprague–Dawley rats (100 ± 20 g) were randomized into four groups. Each group included twelve rats. These groups included (I) a bipedal group, (II) a neck forward flexion group, (III) a neck forward flexion group treated with ISO (20 mg/kg/day), and (IV) a neck forward flexion group treated with ISO (40 mg/kg/day). In accordance with previous research[27], bipedal rats were established by tail and forelimb amputation close to the shoulder joint under general anesthesia. During amputation surgery, 0.5 mg/kg morphine was administered subcutaneously to alleviate the pain caused by the procedure. Six hours post-surgery, another 0.25 mg/kg of morphine was administered subcutaneously. Starting from the second day post-surgery, 0.1 mg/kg meloxicam was administered subcutaneously once daily for 3 days. The heart rate, respiration, blood pressure, body temperature, and visible mucous membrane color of the rats were monitored postsurgery. Wound bleeding, food intake, and water consumption were recorded for 1 week after surgery. One week after amputation, the bipedal rat's neck was kept in anterior flexion of 30° using an elastic splint and medical tape. Over the 8-week experiment, the length of the splint was adjusted as the rats grew. The rats in the treatment group were treated once daily by gavage with ISO (20 mg/kg or 40 mg/kg). The dose of ISO was the same as that used in a previous study[21,28]. After the 8-week experiment was completed, all the rats were euthanized via carbon dioxide asphyxiation following anesthesia. After eight weeks, the cervical disc degeneration models were evaluated using lateral cervical radiographs. After that, the rats were sacrificed, and the integral cervical discs were collected for histochemical and immunohistochemical examination. In the experiment, the smallest incision feasible was made to reduce surgical trauma, and continuous pain relief was provided rather than just a single postoperative morphine dose. Pain levels and behavior were monitored throughout the surgery and feeding phases. If the rats exhibited any signs of distress, intolerance, or severe pain, humane measures were promptly taken, and the animals were removed from the study.

Histological and immunohistochemistry (IHC) examination

The cervical intervertebral discs, including C4–C5, C5–C6, and C6–C7, were resected and dissected microscopically[29]. The IVD tissues were fixed and decalcified using 4% paraformaldehyde and 10% EDTA

solutions, respectively. The paraffin-embedded samples were then cut into 4-μm-thick sections and dehydrated with different concentrations of ethanol and xylene. Finally, a hematoxylin–eosin (H&E) staining kit was used for histological assessment. For the immunohistochemistry study, the sections were deparaffinized and blocked with 10% goat serum. The primary antibodies, including those against cleaved-caspase3 (cat. no. AF7022, Affinity, USA, 1:150 dilution), SRC (cat. no. AF3241, Affinity, USA, 1:150 dilution) and ROS (cat. no. AF0016, Affinity, USA, 1:150 dilution), were reacted overnight at 4 °C. Then, the sections were incubated with goat anti-rabbit secondary antibody (cat. no. BA1039, Boster, China) for 40 min. DAB was used to stain the immunostained samples.

Cell culture

C28/I2 cells were grown in DMEM (Gibco, Germany) supplemented with 10% FBS (Gibco). As described in previous research, cells with or without isorhamnetin (Solarbio Biotechnology, Beijing, China) in medium were cultured in a pressurizing device. A specially designed pressure-loading culture system (see diagram) was used, which can produce a constant hydrostatic pressure inside a sealed culture chamber. The gas was sterilized using a filtration device to maintain sterile conditions. The pressure was continuously monitored and automatically regulated by a microcontroller feedback system to ensure stability throughout the experiment. Moreover, the temperature (37 °C), humidity, and CO_2 concentration were maintained at standard cell culture conditions. To mimic physiological compression and investigate the regulatory effects of hydrostatic pressure under pathological yet nondamaging mechanical conditions, a continuous static pressure of 0.5 MPa was applied for 24 h in the following experiments.

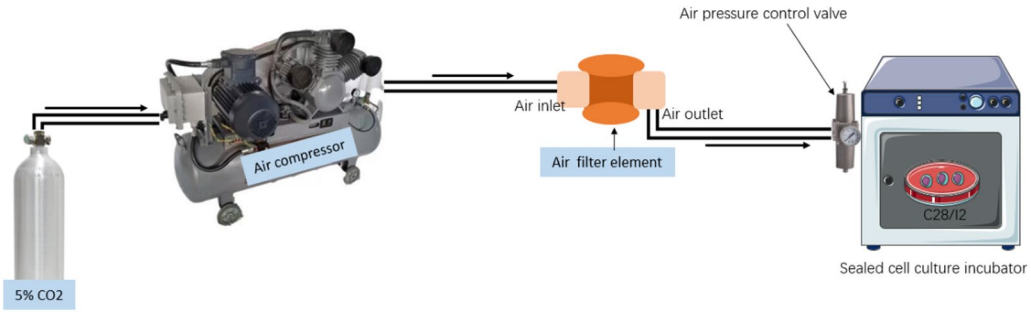

Diagram: Working process of the static pressurized cell culture device.

Cell viability assays

C28/I2 cells (5×10^4 cells/well) were cultured as described above. The growth of chondrocytes cocultured with ISO (Solarbio) was tested with a cell counting kit-8 (Sigma, USA). The optical density at 450 nm was measured using a microplate reader (Thermo, USA).

Western blotting

The cells were interfered with and lysed, and the total protein was collected. Thirty micrograms of protein samples were separated by electrophoresis and then blotted onto PVDF membranes. Primary antibodies against cleaved-caspase3 (cat. no. AF7022, Affinity), SRC (cat. no. AF3241, Affinity), ROS (cat. no. AF0016, Affinity), Bcl-2 (cat. no. AF6139, Affinity), Bax (cat. no. AF0120, Affinity), FOXO1 (cat. no. AF6416, Affinity), p-FOXO1 (cat. no. AF3416, Affinity) and β-actin (cat. no. AF7018, Affinity) were added for incubation overnight at 4 °C. Afterward, the membranes were incubated with an HRP-labeled secondary antibody (1:1500 dilution, Boster, China). The bands were detected using a chemiluminescence imager and analyzed in ImageJ.

Flow cytometric analysis

A flow type reagent kit (Elabscience, Wuhan, China) was used for apoptosis analysis by flow cytometry (BD Biosciences, USA). Specifically, ISO and cells were cocultured in a 6-well plate, after which 5 μl of propidium iodide (PI) solution and 5 μl of Annexin V-FITC were added for staining in the dark for 10 min at room temperature. Finally, apoptosis was detected and analyzed.

Immunocytofluorescence

The cells were spread on a laser confocal Petri dish according to the instructions, and the dish was removed after drug intervention. After fixation using paraformaldehyde, primary and fluorescent secondary antibodies were sequentially incubated with the cells, and, the fluorescence images were then observed on a laser confocal microscope (Carl Zeiss, Germany).

Molecular docking and molecular simulation dynamics

The protein structure database was used to extract essential protein structures from the protein–protein interaction network, and PyMOL software was subsequently used to eliminate ligands and water molecules. PubChem, a comprehensive chemical structure and molecular bioactivity database, was accessed to download

the sdf files of important components. The binding affinities between the compounds and the target protein were evaluated using AutoDock Vina 1.1.2 software, and the docking outcomes were visualized with Discovery Studio. Gromacs 2022 was selected as the software for molecular dynamics simulations, utilizing the Amber14sb force field for the protein and Gaff2 for the ligand. The system incorporates a single point charge (SPC) water model and creates a periodic boundary water box measuring 1.2 nm. To compute long-range electrostatic interactions, the particle–mesh Ewald (PME) method is used, while the Monte Carlo technique is employed for ion placement to ensure the system's overall charge balance by adding appropriate amounts of sodium and chloride ions.

Statistical analysis

The data are shown as the mean ± standard deviation. Statistical analysis was performed using GraphPad Prism v8 software. The primary statistical methods employed were one-way analysis of variance (ANOVA) and Bonferroni's multiple comparison test. A p value of less than 0.05 was considered to indicate a statistically significant difference.

Results

Analysis of the molecular target network of ISO against IDD development

Astragalus has been shown to effectively increase the proliferative vitality of chondrocytes and inhibit IDD[30,31]. A Venn diagram was constructed, which indicated that the number of overlapping targets for Astragalus and IDD was 176 (Fig. 1A). Isorhamnetin, a biologically active saponin in Astragalus, has medicinal potential against IDD (Fig. 1B). The potential common targets of isorhamnetin and IDD were further analyzed. A Venn diagram revealed 350 disease targets closely related to the development of IDD in the database (Fig. 1C,D). Twenty potential molecular targets were obtained by further summarizing and comparing ISO and IDD. SRC, AKT1, and PIK3R1 (Fig. 1E,F) were found to be potential molecular targets of ISO in preventing IDD development.

ISO improved the apoptosis of rat intervertebral disc chondrocytes

Previous research has demonstrated that prolonged exposure to excessive mechanical stress accelerates the degeneration of intervertebral discs[27]. After 73 days of treatment across all the groups, the intervertebral discs were collected for histological analysis (Fig. 2A). HE staining revealed that compared with the bipedal group, the cervical flexion group exhibited a disorganized and decreased arrangement of chondrocytes (Fig. 2B). Oral administration of 25 and 50 mg/kg ISO reduced chondrocyte apoptosis caused by sustained mechanical pressure, improved histological damage, and decreased cartilage endplate degeneration induced by mechanical loading in rats. These findings suggest that ISO may have therapeutic potential for treating and managing IDD.

ISO promoted chondrocyte proliferation and ameliorated mechanical loading-induced apoptosis of CEP chondrocytes

Immunohistochemistry of rat intervertebral discs revealed that 25 mg/kg and 50 mg/kg ISO inhibited the abnormal stress-induced increase in chondrocyte cleaved-caspase3 activity (Fig. 3A,B). To evaluate the cytotoxicity of ISO and its effect on chondrocyte apoptosis, cell viability was assayed using a CCK-8 kit. As shown in Fig. 3D, no apparent cytotoxicity was observed in the groups treated with ISO at concentrations less than 20 μM after 24 h of coculture with chondrocytes. However, the cell viability gradually decreased under exposure to higher concentrations (20–80 μM) of ISO. For further experiments, 5 μM and 20 μM were selected as the low and high concentrations of ISO, respectively. In the presence of stress interventions, cell viability decreased with time. ISO (5 μM and 20 μM) effectively ameliorated the stress-induced reduction in cell viability (Fig. 3E). Next, we investigated the effects of ISO on mechanical loading-induced chondrocyte apoptosis. ISO increased the protein expression levels of antiapoptotic factors, such as Bcl-2 (Fig. 3F,G), and decreased those of apoptosis-related factors, such as Bax, caspase3, and cleaved-caspase3 (Fig. 3F,H,I). Flow cytometry (Fig. 3J–K) revealed that ISO decreased the apoptosis rate of chondrocytes under a mechanical loading of 0.5 MPa. Immunofluorescence staining revealed that 5 μM and 20 μM ISO inhibited the abnormal stress-induced increase in cleaved-caspase3 activity in chondrocytes (Fig. 3L,M). Thus, the protective activity of ISO against mechanical loading-induced degeneration of CEP might be associated with the inhibition of chondrocyte apoptosis.

ISO and SRC exhibit strong affinity and binding capabilities

To investigate the affinity characteristics of ISO and SRC in greater detail, molecular docking and kinetic experiments involving molecular simulations were conducted. The free energy of binding of compound ISO to protein SRC was − 12.8 kcal mol., and the compound bound to 3 amino acid residues (THR-245, VAL-247, GLU-149) of the active protein, indicating that ISO and ARC were compactly bound and had a strong binding capacity (Fig. 4A). The RMSD values for ISO and SRC remained consistently low during the reaction phase, remaining below 2 Å, which suggests that the system achieved a stable state with minimal alterations in protein structure (Fig. 4B–D). Single-site energy (SSE) is used to assess the energy condition of the ISO and SRC composite system within a static framework, demonstrating greater stability of the complex (Fig. 4E,G). The RMSF indicates the variability or movement of atoms or residues in a protein throughout the simulation. As shown in Fig. 4F, the lower RMSF values observed in the ISO simulations than in the SRC simulations suggest that the residues in the complex are more stable. The formation of these hydrogen bonds indicates that ISO binds well to the protein SRC.

ISO reduced the apoptosis of CEP chondrocytes caused by mechanical loading by modulating the SRC/FOXO1 signaling pathway

Based on the docking results of drug and protein molecules, we focused our research on the SRC/FOXO1 signaling pathway. Immunohistochemical analysis of rat intervertebral discs revealed that ISO reduced SRC

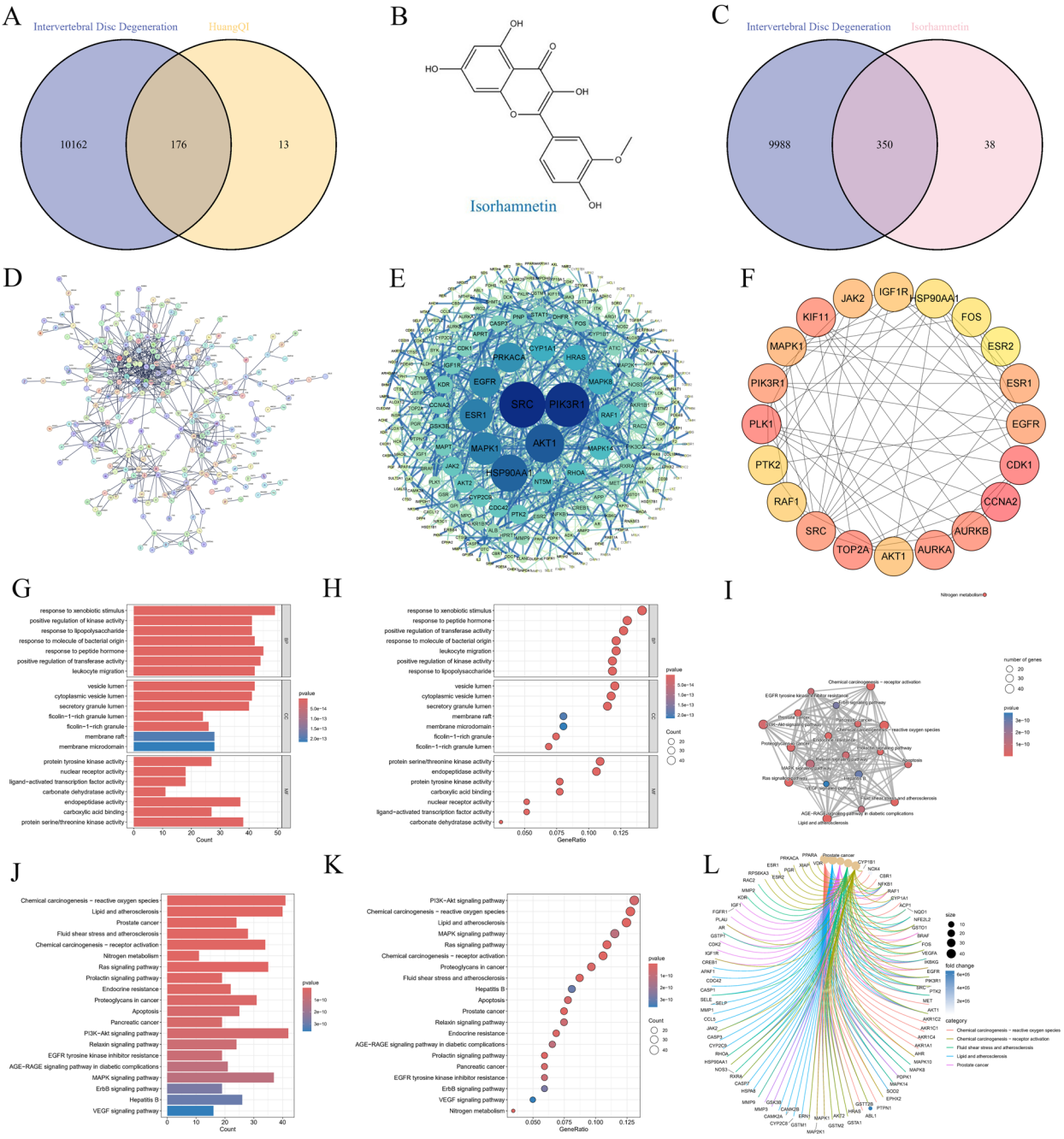

Fig. 1. Mapping of the protein target network of ISO against IDD development. (**A**) Venn diagram of the molecular targets of HuangQi and IDD. (**B**) Chemical structure of isorhamnetin. (**C**) Venn diagram of AST and IDD molecular targets. (**D**–**F**) Summary of the potentially valuable protein targets between ISO and IDD. (**G**,**H**) GO enrichment analysis of isorhamnetin and IDD protein targets. (**I**–**L**) KEGG enrichment analysis of isorhamnetin and IDD protein targets. Molecular docking images of AST and PIK3CA. (**E**) Molecular docking images of AST and AKT1.

protein levels (Fig. 5A,B). To further explore the potential link between the ISO-modulated SRC/FOXO1 signaling pathway and chondrocyte apoptosis induced by mechanical loading, we utilized the SRC activator EPQpYEEIPIYL (EPQ). In chondrocytes subjected to mechanical loading, EPQ counteracted the effects of ISO on SRC/FOXO1 signaling, as indicated by decreased phosphorylation of FOXO1. EPQ also partially reversed the protective effect of AST on the expression of apoptosis-related proteins (Fig. 5C–H). Furthermore, EPQ diminished the inhibitory effect of ISO on chondrocyte apoptosis, as shown by flow cytometry (Fig. 5K,L). Immunofluorescence staining revealed that ISO reduced the fluorescence intensity of cleaved-caspase3 induced by mechanical stress (Fig. 5I,J). Therefore, ISO appears to activate the SRC/FOXO1 signaling pathway to prevent chondrocyte apoptosis caused by mechanical loading.

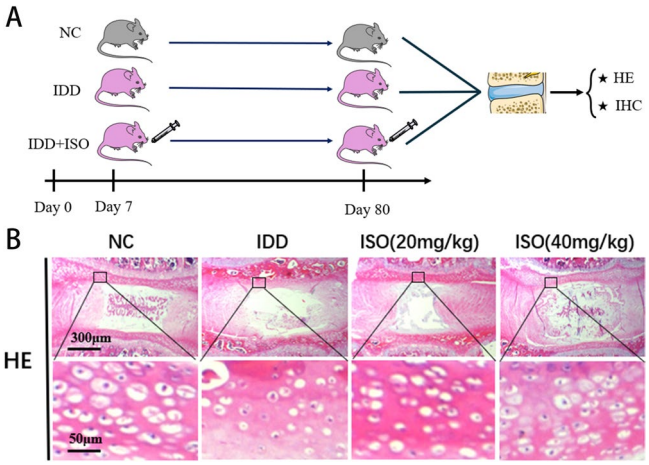

Fig. 2. ISO improved the apoptosis of rat intervertebral disc chondrocytes. (**A**) Flow chart of the in vivo rat experiment. (**B**) HE staining of isolated cervical intervertebral discs.

ISO inhibits mechanical loading-induced chondrocyte apoptosis by modulating the ROS-dependent SRC/FOXO1 signaling pathway

To further investigate the potential relationship between the ISO-induced activation of the SRC/FOXO1 signaling pathway and mechanical loading-induced chondrocyte apoptosis, the ROS activator H2O2 was used. Immunohistochemical experiments were performed to assess ROS levels (Fig. 6A,B). In mechanically loaded chondrocytes, H2O2 inhibited ISO-activated SRC/FOXO1 signaling, as evidenced by decreased FOXO1 phosphorylation and increased SRC expression. The protective effects of ISO on the protein expression of apoptosis-related factors were partially reversed by H2O2 (Fig. 6C–I). In addition, H2O2 attenuated the inhibitory effects of ISO on chondrocyte apoptosis, as detected by flow cytometry (Fig. 6J,K) and immunocytofluorescence (Fig. 6L,M). Thus, ISO activated the ROS-dependent SRC/FOXO1 signaling pathway to inhibit mechanical loading-induced chondrocyte apoptosis.

Discussion

As one of the leading causes of chronic neck pain and cervical kyphosis, IDD is a global burden associated with health care concerns and socioeconomic costs[32,33]. Key characteristics of the pathological changes associated with IDD include the thinning of cartilage endplates, disorganization of the annulus fibrosus, and degeneration of the nucleus pulposus. Although new progress has been made in the surgical modalities of IDD, the currently available interventions are still unsatisfactory.

In general, healthy mechanical loading contributes to the maintenance of IVD mechanical microenvironment homeostasis. Spinal dynamic loading at a physiological frequency is beneficial to IVD nutrient metabolism and matrix balance[34,35]. Furthermore, another study revealed that a threshold exists for detrimental mechanical loading, including the hydrostatic or dynamic pressure[36]. The risk factors contributing to the pathogenesis of IDD vary, and the mechanical loading-induced destruction of the IVD has long been thought to be a cause of IDD development[37,38]. Different IVD cells respond differently to dynamic mechanical compression in terms of loading, duration, and frequency in vivo[39]. Many studies have demonstrated that the CEP plays important roles in IVD biomechanical integrity and nutrient exchange[40,41]. As the outermost structure of the IVD, the CEP may be more susceptible to mechanical loading. Previous research has shown that the chondrocyte density in the CEP is decreased in patients with IDD[42]. Static mechanical loading (1.0 MPa) of cultured CEP tissues in vitro can induce apoptosis[17]. Our study revealed that 0.5 MPa mechanical loading could increase the level of apoptosis in C28/I2 cells, as indicated by the downregulation of Bcl-2 expression and upregulation of cleaved-caspase3 and Bax expression. In addition, increased chondrocyte apoptosis was observed in the rat cervical CEP due to abnormal mechanical loading from neck flexion. To further explore the pathological mechanisms through which mechanical stress leads to intervertebral disc compression, this study utilized a bipedal rat model of intervertebral disc degeneration. Because these rats walk upright on two legs, their spines experience continuous axial loading, resulting in progressive disc dehydration, loss of extracellular matrix, endplate degeneration, and activation of inflammation—characteristics closely resembling the degeneration caused by biomechanical overload in human intervertebral disc degeneration (IDD). In this study, ISO notably reduced chondrocyte apoptosis and moderately mitigated intervertebral disc degeneration in the bipedal rat model.

The SRC/FOXO1 signaling pathway is involved in the regulation of gene transcription and protein translation and modification and plays a crucial role in the regulation of apoptosis[43,44]. SRC, as a nonreceptor tyrosine kinase, activates the PI3K/AKT pathway and further phosphorylates FOXO1, causing its retention in the cytoplasm and loss of transcriptional activity, thereby inhibiting FOXO1-regulated apoptotic gene expression[45,46]. One study reported that FOXO1 interacts with the metastasis-related molecule SRC to facilitate apoptosis. In chondrocytes, the SRC inhibitor PP2 reduced apoptosis[46]. Furthermore, the Src kinase family inhibitor AZD0530 (saracatinib) has been shown to be effective at treating experimental osteoarthritis in mice[47]. In our current research, we

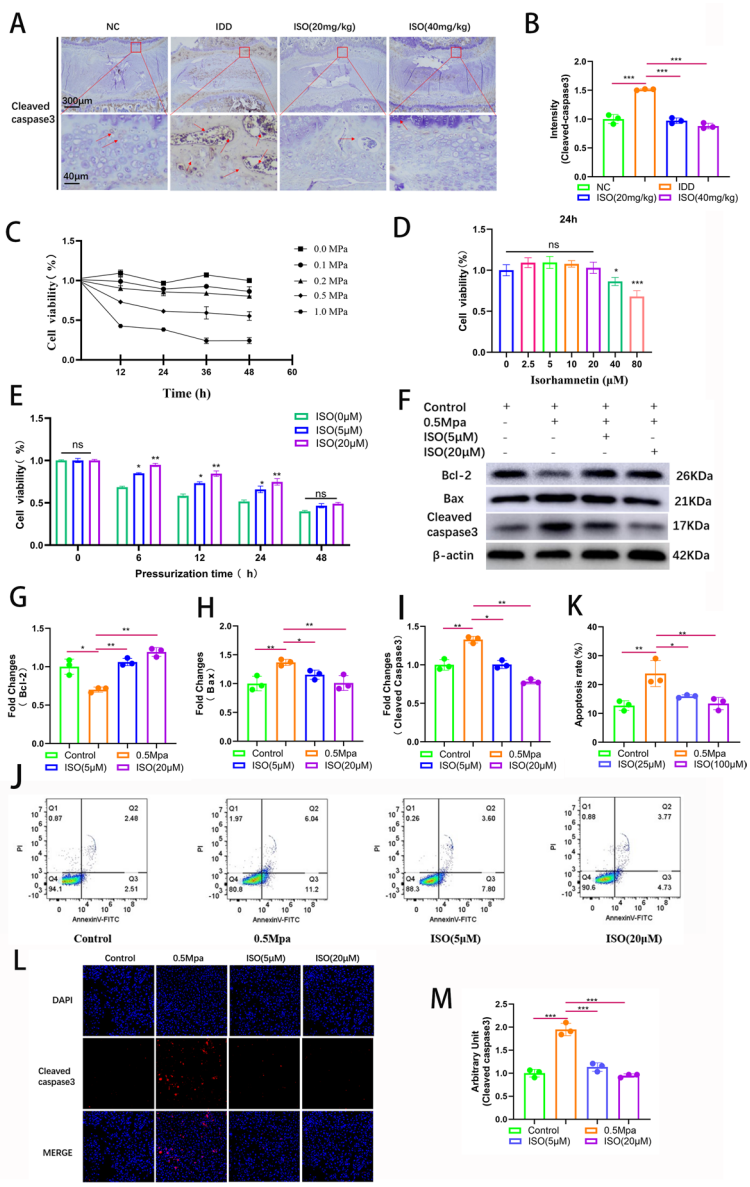

Fig. 3. The role of ISO in mechanical loading-induced chondrocyte apoptosis. (**A**,**B**) Immunohistochemical results showing cleaved-caspase3 in rat intervertebral discs. (**C**) Effects of static pressure at different intensities on chondrocytes. (**D**) CCK-8 assays to determine the cytotoxicity of ISO (0, 2.5, 5, 10, 20, 40 and 80 μM) on C28/I2 cells. (**E**) CCK-8 assays to detect the effects of ISO (0, 5 and 20 μM) on cell viability at different intervention times. (**F**–**G**) Detection of the apoptosis rate by flow cytometry. (J–K) Western blotting assays to assess the expression of Bcl-2 (**F**,**G**), Bax (**F**,**H**), and cleaved-caspase3 (**F**,**I**). (**L**,**M**) Immunocytofluorescence evaluation of cleaved-caspase3 expression in each group. $^{*}P < 0.05$, $^{**}P < 0.01$. ISO (20 mg/kg and 40 mg/kg), the forward flexed neck group treated with ISO (20 and 40 mg/kg/day, respectively); 0.5 MPa, cells treated with 0.5 MPa of mechanical pressure; ISO (5 μM and 20 μM), cells treated with 0.5 MPa of mechanical pressure + 5 μM and 20 μM of ISO, respectively.

observed that SRC expression was elevated while FOXO1 expression was reduced in rats subjected to cervical flexion. Additionally, mechanical loading at 0.5 MPa decreased the phosphorylation level of FOXO1 and increased the expression levels of apoptosis-related proteins such as Bax and cleaved-caspase3 in C28/I2 cells.

Stress-induced reactive oxygen species (ROS) increase the kinase activity of SRC by oxidizing its cysteine residues and disrupting its autoinhibitory structure. Once activated, SRC phosphorylates downstream targets and suppresses the transcriptional activity of FOXO1[48]. As a result, phosphorylated FOXO1 is unable to trigger the transcription of antioxidant genes (such as SOD), diminishing the ability of cells to eliminate ROS[49]. Additionally, SRC stimulates NADPH oxidase activity, leading to increased ROS production and the establishment of a positive feedback loop. Research has shown that in pathological conditions such as tumors, prolonged SRC activation results in ROS accumulation, surpassing the antioxidant defense threshold and causing DNA damage and mitochondrial dysfunction[50]. Moreover, integrin-dependent Src contributes to ROS

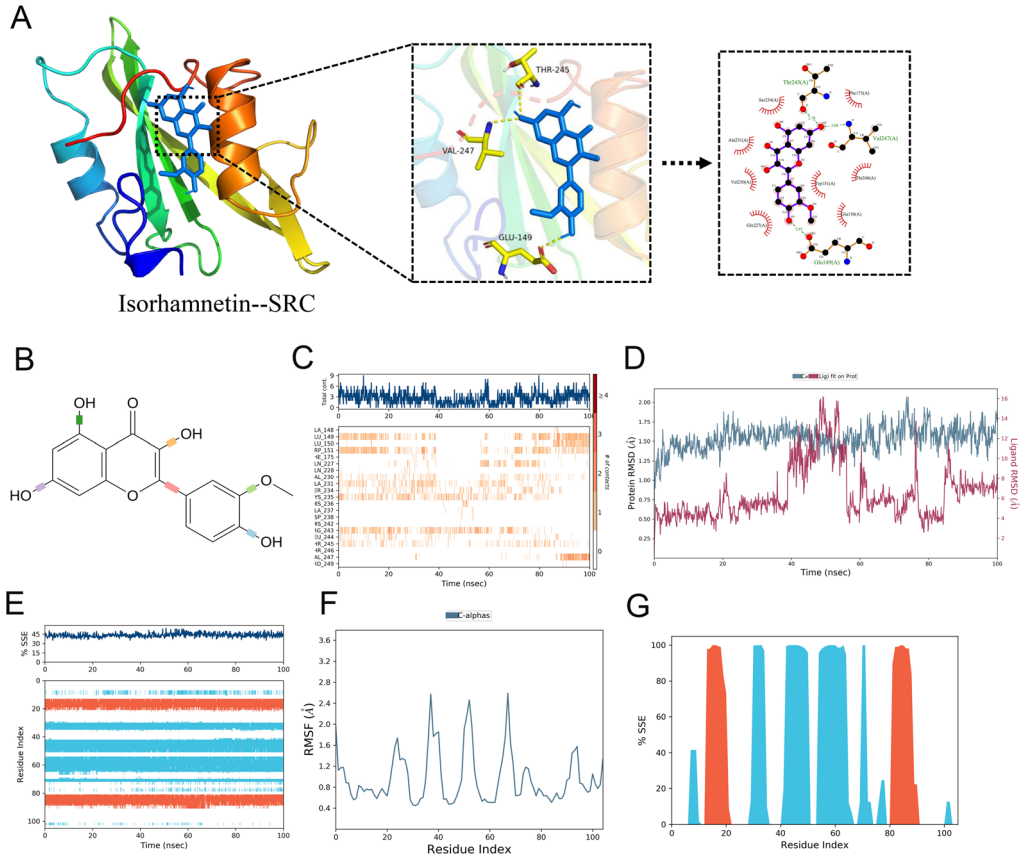

Fig. 4. Molecular docking and molecular simulation kinetic results for ISO and SRC. (**A**) Molecular docking data from ISO and SRC. (**B**) ISO and SRC combined static structure. (**C–G**) Molecular simulation kinetic results for ISO and SRC.

accumulation and the degradation of the extracellular matrix in osteoarthritic chondrocytes[51]. Our study verified that ROS levels were elevated in chondrocytes subjected to mechanical stress. Moreover, ISO may influence the SRC/FOXO1 signaling pathway by targeting it in a ROS-dependent manner.

ISO is a flavonoid known for its anti-inflammatory, antitumor, and antioxidant effects[52,53]. Research has shown that ISO can significantly decrease the production of reactive oxygen species (ROS) and the mitochondrial membrane potential in mouse macrophages that have been exposed to hydrogen peroxide. It may also slow the progression of osteoarthritis induced by IL-1β[23]. Previous studies have indicated that ISO has stronger protective effects on bone mineralization, metabolism, and oxidative stress in bone tissue[54]. Recent findings suggest that ISO enhances the differentiation and migration of osteoblasts by influencing bone morphogenetic protein 2 (BMP2)/mothers against decapentaplegic homolog 2 (Smad) signaling pathway[55]. Furthermore, ISO has been shown to improve the pathological development of colon cancer by regulating SRC kinase activity in colon cancer cells. Our study supports these findings, showing that ISO inhibits the ROS/SRC/FOXO1 pathway by reducing excessive mechanical load-induced apoptosis both in vivo and in vitro. Activation of the ROS/SRC/FOXO1 signaling pathway significantly diminished the protective effects of ISO on C28/I2 cells subjected to mechanical overload.

Bipedal rats are subjected to sustained axial loading on the spine because of upright posture, which leads to progressive disc dehydration, loss of extracellular matrix, endplate degeneration, and inflammatory activation—features that closely resemble the biomechanical overload–driven degeneration observed in human IDD. Therefore, this model enables the investigation of disc degeneration under chronic mechanical stress in vivo[27]. Nevertheless, there are several limitations associated with using animal models. It is anticipated that future studies will focus on models of intervertebral disc explant culture and mechanical stimulation in vitro to minimize animal use and their distress.

Furthermore, we recognize the inherent limitations of the current ISO treatment for intervertebral disc degeneration. Although ISO reduced some degenerative symptoms, the degree of structural healing and functional improvement observed in our study was not complete. Thus, the therapeutic effectiveness of ISO should be viewed cautiously, and additional research is needed before definitive clinical conclusions can be made.

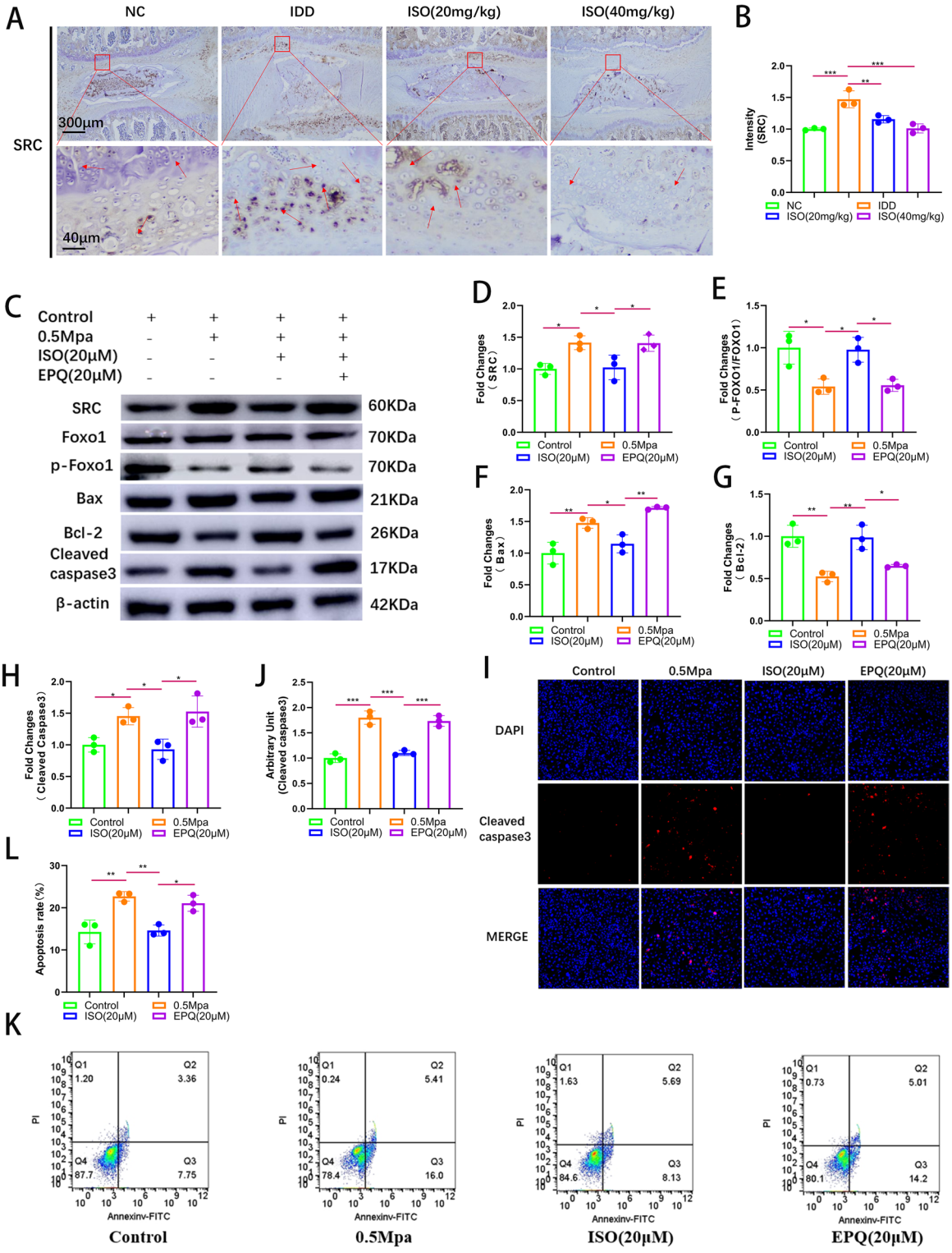

Fig. 5. The SRC activator EPQ neutralized the protective effects of ISO on mechanical loading-induced chondrocyte apoptosis. Immunohistochemistry of rat intervertebral discs showing that ISO promoted the protein expression of SRC (**A**,**B**). Western blotting assays showing the expression of SRC (**C**,**D**), p-FOXO1 (**C**,**E**), Bcl-2 (**C**,**G**), Bax (**C**,**F**), and cleaved-caspase3 (**C**,**H**). (**I**–**J**) Detection of the apoptosis rate by flow cytometry. (**K**,**L**) Immunofluorescence staining to evaluate the expression of cleaved-caspase3. $^{*}P < 0.05$, $^{**}P < 0.01$. 0.5 MPa, cells treated with 0.5 MPa of mechanical loading; ISO (20 μM and 5 μM), cells treated with 0.5 MPa of mechanical loading + 5 μM and 20 μM of ISO, respectively.

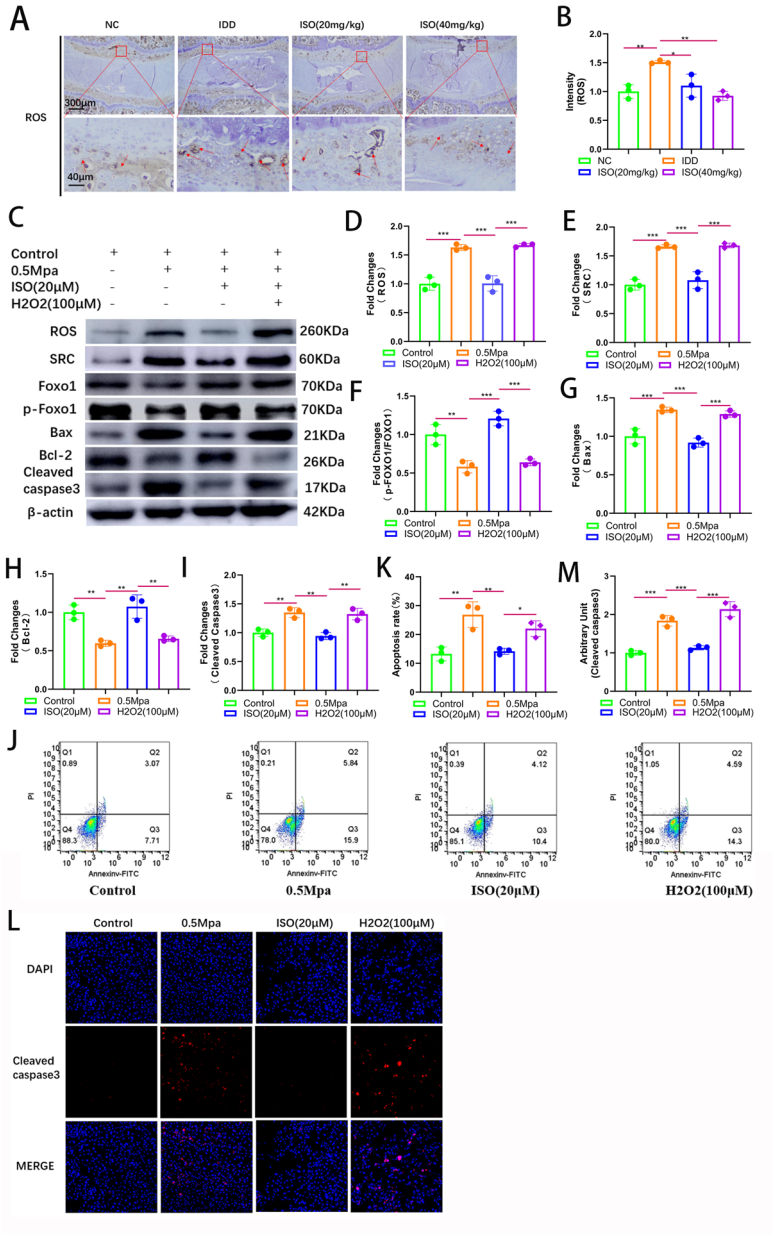

Fig. 6. ISO inhibits mechanical loading-induced chondrocyte apoptosis by modulating the ROS-dependent SRC/FOXO1 signaling pathway. Immunohistochemistry of rat intervertebral discs showing that ISO promoted the protein expression of ROS (**A**,**B**). Western blotting assays showing the expression of ROS (**C**,**D**), SRC (**C**,**E**), p-FOXO1 (**C**,**F**), Bax (**C**,**G**), Bcl-2 (**C**,**H**), and cleaved-caspase3 (**C**,**I**). (**J**,**K**) Detection of the apoptosis rate by flow cytometry. (**L**,**M**) Immunofluorescence staining to evaluate the expression of cleaved-caspase3. *P < 0.05, **P < 0.01. 0.5 MPa, cells treated with 0.5 MPa of mechanical loading; ISO (20 μM and 5 μM), cells treated with 0.5 MPa of mechanical loading + 5 μM and 20 μM of ISO, respectively.

Conclusion

In this study, we found that excessive mechanical loading was associated with increased chondrocyte apoptosis both in vivo and in vitro. Mechanical stress may activate the SRC/FOXO1 signaling pathway. ISO protected against mechanical loading-induced chondrocyte apoptosis and restored cervical curvature in rats. However, activation of the ROS/SRC/FOXO1 signaling pathway by EPQpYEEIPIYL and H2O2 attenuated the biological effects of ISO on mechanical loading-treated C28/I2 cells. Therefore, ISO inhibits mechanical loading-induced chondrocyte apoptosis by modulating the ROS-dependent SRC/FOXO1 signaling pathway.

Data availability

This article contains the data used to support the results of this study. Further data will be provided by Yadong Yang upon request.

Received: 14 August 2025; Accepted: 12 January 2026
Published online: 13 January 2026

References

1. Vos, T. et al. Years lived with disability (YLDs) for 1160 sequelae of 289 diseases and injuries 1990–2010: a systematic analysis for the global burden of disease study 2010. *Lancet* **380**, 2163–2196. https://doi.org/10.1016/S0140-6736(12)61729-2 (2012).
2. Xin, J. et al. Treatment of intervertebral disc degeneration. *Orthop. Surg.* **14**, 1271–1280. https://doi.org/10.1111/os.13254 (2022).
3. Brinjikji, W. et al. Systematic literature review of imaging features of spinal degeneration in asymptomatic populations. *AJNR Am. J. Neuroradiol.* **36**, 811–816. https://doi.org/10.3174/ajnr.A4173 (2015).
4. Senck, S. et al. Visualization of intervertebral disc degeneration in a cadaveric human lumbar spine using microcomputed tomography. *J. Anat.* **236**, 243–251. https://doi.org/10.1111/joa.13105 (2020).
5. Ashinsky, B., Smith, H. E., Mauck, R. L. & Gullbrand, S. E. Intervertebral disc degeneration and regeneration: a motion segment perspective. *Eur. Cell. Mater.* **41**, 370–380. https://doi.org/10.22203/eCM.v041a24 (2021).
6. Ashinsky, B. G. et al. Intervertebral disc degeneration is associated with aberrant endplate remodeling and reduced small molecule transport. *J. Bone Min. Res.* **35**, 1572–1581. https://doi.org/10.1002/jbmr.4009 (2020).
7. DeLucca, J. F. et al. Human cartilage endplate permeability varies with degeneration and intervertebral disc site. *J. Biomech.* **49**, 550–557. https://doi.org/10.1016/j.jbiomech.2016.01.007 (2016).
8. Ge, Q. et al. Chlorogenic acid retards cartilaginous endplate degeneration and ameliorates intervertebral disc degeneration via suppressing NF-κB signaling. *Life Sci.* **274**, 119324. https://doi.org/10.1016/j.lfs.2021.119324 (2021).
9. Su, Q. et al. Association and histological characteristics of endplate injury and intervertebral disc degeneration in a rat model. *Injury* **52**, 2084–2094. https://doi.org/10.1016/j.injury.2021.05.034 (2021).
10. Han, Y. et al. Oxidative damage induces apoptosis and promotes calcification in disc cartilage endplate cell through ROS/MAPK/NF-κB pathway: implications for disc degeneration. *Biochem. Biophys. Res. Commun.* **516**, 1026–1032. https://doi.org/10.1016/j.bbrc.2017.03.111 (2019).
11. Zhang, F., Zhao, X., Shen, H. & Zhang, C. Molecular mechanisms of cell death in intervertebral disc degeneration (Review). *Int. J. Mol. Med.* **37**, 1439–1448. https://doi.org/10.3892/ijmm.2016.2573 (2016).
12. Ding, F., Shao, Z. & Xiong, L. Cell death in intervertebral disc degeneration. *Apoptosis* **18**, 777–785. https://doi.org/10.1007/s10495-013-0839-1 (2013).
13. Ariga, K. et al. The relationship between apoptosis of endplate chondrocytes and aging and degeneration of the intervertebral disc. *Spine (Phila Pa. 1976).* **26**, 2414–2420 (2001).
14. Wang, B. et al. Mechanosensitive ion channel Piezo1 activated by matrix stiffness regulates oxidative Stress-Induced senescence and apoptosis in human intervertebral disc degeneration. *Oxid. Med. Cell. Longev.* **2021**, 8884922. https://doi.org/10.1155/2021/8884922 (2021).
15. Zhang, X. B. et al. Targeted therapy for intervertebral disc degeneration: inhibiting apoptosis is a promising treatment strategy. *Int. J. Med. Sci.* **18**, 2799–2813. https://doi.org/10.7150/ijms.59171 (2021).
16. Vergroesen, P. P. A. et al. Mechanics and biology in intervertebral disc degeneration: a vicious circle. *Osteoarthr. Cartil.* **23**, 1057–1070. https://doi.org/10.1016/j.joca.2015.03.028 (2015).
17. Ariga, K. et al. Mechanical stress-induced apoptosis of endplate chondrocytes in organ-cultured mouse intervertebral discs: an ex vivo study. *Spine (Phila Pa 1976)* **28**, 1528–1533 (2003).
18. Zhu, Y. et al. NDP52 deficiency accelerates chondrocyte degeneration through promoting pathogenic mitochondrial ROS via reverse electron transport. *Redox Biol.* **85**, 103747. https://doi.org/10.1016/j.redox.2025.103747 (2025).
19. Yu, S. M. & Kim, S. J. Endoplasmic reticulum stress (ER-stress) by 2-deoxy-D-glucose (2DG) reduces cyclooxygenase-2 (COX-2) expression and N-glycosylation and induces a loss of COX-2 activity via a Src kinase-dependent pathway in rabbit articular chondrocytes. *Exp. Mol. Med.* **42**, 777–786 (2010).
20. Akasaki, Y. et al. FoxO transcription factors support oxidative stress resistance in human chondrocytes. *Arthritis Rheumatol.* **66**, 3349–3358. https://doi.org/10.1002/art.38868 (2014).
21. Zhou, F. et al. Isorhamnetin attenuates osteoarthritis by inhibiting osteoclastogenesis and protecting chondrocytes through modulating reactive oxygen species homeostasis. *J. Cell. Mol. Med.* **23**, 4395–4407. https://doi.org/10.1111/jcmm.14333 (2019).
22. Tsai, S. W., Lin, C. C., Lin, S. C., Wang, S. P. & Yang, D. H. Isorhamnetin ameliorates inflammatory responses and articular cartilage damage in the rats of monosodium iodoacetate-induced osteoarthritis. *Immunopharmacol. Immunotoxicol.* **41**, 504–512. https://doi.org/10.1080/08923973.2019.1641723 (2019).
23. Li, J. et al. Isorhamnetin inhibits IL-1β–induced expression of inflammatory mediators in human chondrocytes. *Mol. Med. Rep.* **16**, 4253–4258. https://doi.org/10.3892/mmr.2017.7041 (2017).
24. Liu, X. R., Li, S. F., Mei, W. Y., Liu, X. D. & Zhou, R. B. Isorhamnetin downregulates MMP2 and MMP9 to inhibit development of rheumatoid arthritis through SRC/ERK/CREB pathway. *Chin. J. Integr. Med.* **30**, 299–310. https://doi.org/10.1007/s11655-023-3753-6 (2024).
25. Guo, Z. et al. Isorhamnetin attenuates isoproterenol-induced myocardial injury by reducing ENO1 (Alpha-Enolase) in cardiomyocytes. *Antioxidants (Basel)* **14**. (2025). https://doi.org/10.3390/antiox14050579
26. Eck, M. J., Shoelson, S. E. & Harrison, S. C. Recognition of a high-affinity phosphotyrosyl peptide by the Src homology-2 domain of p56lck. *Nature.* **362**, 87–91 (1993).
27. Lai, J. et al. Apoptosis of endplate chondrocytes in cervical kyphosis is associated with chronic forward flexed neck: an in vivo rat bipedal walking model. *J. Orthop. Surg. Res.* **16** https://doi.org/10.1186/s13018-020-02124-4 (2021).
28. Chen, Y. et al. Isorhamnetin attenuates renal interstitial fibrosis by targeting TWEAK/Fn14-mediated epithelial-mesenchymal transition. *Front. Immunol.* **16**, 1649327. https://doi.org/10.3389/fimmu.2025.1649327 (2025).
29. Zhou, C. et al. Intervertebral range of motion characteristics of normal cervical spinal segments (C0-T1) during in vivo neck motions. *J. Biomech.* **98**, 109418. https://doi.org/10.1016/j.jbiomech.2019.109418 (2020).
30. Chen, K. et al. Systematic pharmacology and experimental validation to reveal the alleviation of astragalus membranaceus regulating ferroptosis in osteoarthritis. *Drug Des. Dev. Ther.* **18**, 259–275. https://doi.org/10.2147/DDDT.S441350 (2024).
31. Rahman, M. M. et al. Chondroprotective effects of a standardized extract (KBH-JP-040) from *Kalopanax pictus*, *Hericium erinaceus*, and *Astragalus membranaceus* in experimentally induced in vitro and in vivo osteoarthritis models. *Nutrients* **10**. (2018). https://doi.org/10.3390/nu10030356
32. Machino, M. et al. Cervical disc degeneration is associated with a reduction in mobility: A cross-sectional study of 1211 asymptomatic healthy subjects. *J. Clin. Neurosci.* **99**, 342–348. https://doi.org/10.1016/j.jocn.2022.03.035 (2022).
33. Theodore, N. Degenerative cervical spondylosis. *N. Engl. J. Med.* **383**, 159–168. https://doi.org/10.1056/NEJMra2003558 (2020).
34. Wuertz, K. et al. In vivo remodeling of intervertebral discs in response to short- and long-term dynamic compression. *J. Orthop. Res.* **27**, 1235–1242. https://doi.org/10.1002/jor.20867 (2009).
35. Chan, S. C. W., Ferguson, S. J. & Gantenbein-Ritter, B. The effects of dynamic loading on the intervertebral disc. *Eur. Spine J.* **20**, 1796–1812. https://doi.org/10.1007/s00586-011-1827-1 (2011).
36. MacLean, J. J. et al. Effects of immobilization and dynamic compression on intervertebral disc cell gene expression in vivo. *Spine (Phila Pa. 1976).* **28**, 973–981 (2003).

37. Stokes, I. A. F. & Iatridis, J. C. Mechanical conditions that accelerate intervertebral disc degeneration: overload versus immobilization. *Spine (Phila Pa 1976)* **29**, 2724–2732 (2004).
38. Guehring, T. et al. Stimulation of gene expression and loss of anular architecture caused by experimental disc degeneration—an in vivo animal study. *Spine (Phila Pa 1976)* **30**, 2510–2515 (2005).
39. MacLean, J. J., Lee, C. R., Alini, M. & Iatridis, J. C. The effects of short-term load duration on anabolic and catabolic gene expression in the rat tail intervertebral disc. *J. Orthop. Res.* **23**, 1120–1127 (2005).
40. Grunhagen, T., Shirazi-Adl, A., Fairbank, J. C. T. & Urban, J. P. G. Intervertebral disk nutrition: a review of factors influencing concentrations of nutrients and metabolites. *Orthop. Clin. N. Am.* **42**. (2011). https://doi.org/10.1016/j.ocl.2011.07.010
41. Grunhagen, T., Wilde, G., Soukane, D. M., Shirazi-Adl, S. A. & Urban, J. P. G. Nutrient supply and intervertebral disc metabolism. *J. Bone Jt. Surg. Am.* **88** (Suppl 2), 30–35 (2006).
42. Tomaszewski, K. A. et al. Age- and degeneration-related variations in cell density and glycosaminoglycan content in the human cervical intervertebral disc and its endplates. *Pol. J. Pathol.* **66**, 296–309 (2015).
43. Liu, Y. et al. Exposure to the prenatal enriched environment alters maternal gut microbiota and promotes embryonic neurodevelopment via activating the AHR-Src pathway. *Sci. China Life Sci.* https://doi.org/10.1007/s11427-024-2870-4 (2025).
44. Mazzone, V. et al. Terpenes: natural compounds found in plants as potential senotherapeutics targeting senescent mesenchymal stromal cells and promoting apoptosis. *Stem Cell. Res. Ther.* **16**, 231. https://doi.org/10.1186/s13287-025-04310-9 (2025).
45. Chen, S. et al. TIN2 modulates FOXO1 mitochondrial shuttling to enhance oxidative stress-induced apoptosis in retinal pigment epithelium under hyperglycemia. *Cell. Death Differ.* **31**, 1487–1505. https://doi.org/10.1038/s41418-024-01349-8 (2024).
46. Zhang, T. et al. Type I BODITh photosensitizers with twisted conformation for augmented photodynamic therapy and FOXO1-Involved apoptosis. *Nano Lett.* **25**, 8379–8389. https://doi.org/10.1021/acs.nanolett.5c01663 (2025).
47. Li, K. et al. Tyrosine kinase Fyn promotes osteoarthritis by activating the β-catenin pathway. *Ann. Rheum. Dis.* **77**, 935–943. https://doi.org/10.1136/annrheumdis-2017-212658 (2018).
48. Li, L. F. et al. Inhibition of Src and forkhead box O1 signaling by induced pluripotent stem-cell therapy attenuates hyperoxia-augmented ventilator-induced diaphragm dysfunction. *Transl. Res.* **173** https://doi.org/10.1016/j.trsl.2016.03.011 (2016).
49. Carlomosti, F. et al. Oxidative stress-induced miR-200c disrupts the regulatory loop among SIRT1, FOXO1, and eNOS. *Antioxid. Redox Signal.* **27**, 328–344. https://doi.org/10.1089/ars.2016.6643 (2017).
50. Bohrer, L. R. et al. FOXO1 binds to the TAU5 motif and inhibits constitutively active androgen receptor splice variants. *Prostate* **73**, 1017–1027. https://doi.org/10.1002/pros.22649 (2013).
51. Goldring, M. B. Integrin-dependent recruitment of Src to ROS-producing endosomes in Osteoarthritic cartilage. *Sci. Signal.* **16**, eadj9760. https://doi.org/10.1126/scisignal.adj9760 (2023).
52. Mei, C. et al. Advances in isorhamnetin treatment of malignant tumors: mechanisms and applications. *Nutrients*. **17**. (2025). https://doi.org/10.3390/nu17111853
53. Kong, X. et al. Isorhamnetin ameliorates hyperuricemia by regulating uric acid metabolism and alleviates renal inflammation through the PI3K/AKT/NF-κB signaling pathway. *Food Funct.* **16**, 2840–2856. https://doi.org/10.1039/d4fo04867a (2025).
54. Jiao, H. & Zheng, K. Isorhamnetin ameliorates ovariectomy-induced osteoporosis in female rats by regulating the receptor activator of nuclear factor kappa B ligand, osteoprotegerin, bone morphogenetic protein 2 and runt-related transcription factor 2 signaling pathway. *J. Vet. Med. Sci.* https://doi.org/10.1292/jvms.25-006 (2025).
55. Li, J. et al. Pro-differentiative, Pro-adhesive and Pro-migratory activities of Isorhamnetin in MC3T3-E1 osteoblasts via activation of ERK-dependent BMP2-Smad signaling. *Cell. Biochem. Biophys.* **82**, 3607–3617. https://doi.org/10.1007/s12013-024-01450-2 (2024).

Author contributions

Y.Y. conceptualized this paper. J.L., G.Y., J.H., F.Z., X.H., L.L., J.T., S.W., Y.X., R.W., S.L., J.Z. and Y.G. conducted the experiments and revised the paper. The final version of the paper has been approved by all the authors.

Funding statement

This study was financially supported by the Science and Technology Plan of Jiangxi Health Commission (SKJP_20204484, SKJP_20195368).

Declarations

Competing interests

The authors declare no competing interests.

Additional information

Supplementary Information The online version contains supplementary material available at https://doi.org/10.1038/s41598-026-36249-z.

Correspondence and requests for materials should be addressed to Y.Y.

Reprints and permissions information is available at www.nature.com/reprints.

Publisher's note Springer Nature remains neutral with regard to jurisdictional claims in published maps and institutional affiliations.